Available online at www.sciencedirect.com
SCIENCE DIRECT®
Polymer 45 (2004) 1845–1855
polymer
www.elsevier.com/locate/polymer

Dynamic mechanical and dielectric relaxations in poly(di-*n*-chloroalkylitaconates)

M.J. Sanchis[a], R. Díaz-Calleja[a,*], O. Pelissou[a], L. Gargallo[b], D. Radiç[b]

[a]*Departamento de Termodinámica Aplicada, E.T.S.I.I., Universidad Politécnica de Valencia, Camino de Vera s/n, Apartado 22012, 46071 Valencia, Spain*
[b]*Departamento de Química Física, Facultad de Química, Potificia Universidad Católica de Chile, Casilla 306, Santiago 22, Chile*

Received 6 October 2003; accepted 6 January 2004

Abstract

Dielectric and viscoelastic relaxation measurements have been carried out on poly(2-chloroethyl diitaconate) (PDCEI) and poly(3-chloropropyl diitaconate) (PDCPI) between 123 K and temperatures about 293 K above the glass transition temperatures.

The two polymers exhibit three peaks, a γ-relaxation in the range from 133 to 193 K (at 1 Hz), a broad β-process, in the range from 193 to 293 K and a third peak observed in mechanical measurements at 323 K (PDCEI) and 293 K (PDCPI) probably corresponding to the α dynamic glass transition phenomena. In dielectric measurements, conductive contributions overlap the α-relaxation precluding the observation of peaks at temperatures above room temperature. The apparent activation energies for the γ-relaxation according to the mechanical and dielectric measurements are close to the values derived from the empirical force field molecular mechanics calculations. A comparison is made between the relaxational data of PDCEI and PDCPI by one hand and poly(di-*n*-propyl itaconate) (PDPI) and poly(di-*n*-butyl itaconate) (PDBI) by other. This comparison allows us to conclude the relevant role played by the chlorine atoms not only in the γ relaxations but also in the β relaxations of PDCEI and PDCPI.

Keywords: Poly(itaconates); Dielectric and mechanical relaxations; Molecular mechanics

1. Introduction

Esterification of (2-methylenesuccinic acid) is the usual way to obtain monomers with a variety of structural possibilities. In fact, itaconic acid can be selectively esterified, to obtain mono and diitaconates and the corresponding polymers. This structural versatility gives rise to a wide variety of different polymers. These polymers show a complex relaxational behavior, due to the large number of degrees of freedom of its chain [1–4]. In the case of poly(acrylate)s and poly(methacrylate)s with long chloroalkyl side chains, important relaxation processes are observed at cryogenic temperatures [5]. This is also the case of the corresponding poly(itaconates) with long side chains. In the case of poly(di-*n*-alkyl itaconates), there is an important increasing of the steric hindrance because of the presence of two side groups per repeating unit. These groups originate significative dielectric and mechanical absorptions [1–5] due to the fact that internal librations of dipolar units are still possible. Therefore, the number of relaxations should be higher than in the case of poly(methacrylate)s and poly(acrylate)s. As expected in this type of polymers, dielectric α relaxations are overlapped by strong conductivity and related phenomena.

In this work we have studied the relaxational behavior by dielectric and mechanical techniques of two poly(di-*n*-chloroalkyl itaconate)s i.e. poly(di-2-chloroethyl and poly(di-3-chloropropyl itaconate)s (PDCEI and PDCPI) in a wide range of temperatures and frequencies.

Moreover, in order to elucidate the molecular motions responsible for the lower temperature relaxational processes, via the knowledge of their activation energies, we have carried out conformational calculations. Molecular mechanics can be considered as a powerful tool for analyzing the molecular motions causing secondary relaxations [6,7]. However, in general, for each molecular group in the polymer, there are many available molecular conformations consistent with the same value of the energy. For this reason, in order to simplify calculations in our

* Corresponding author.
E-mail address: rdiazc@ter.upv.es (R. Díaz-Calleja).

0032-3861/$ - see front matter © 2004 Elsevier Ltd. All rights reserved.
doi:10.1016/j.polymer.2004.01.017

molecular mechanics study, and to interpret the results in an easier way, we have used an approach similar to that employed by other authors [8–16], i.e. the use of the model compounds (with one and three molecular units).

2. Experimental section

2.1. Monomer and polymer preparation

2-Chloroethyl and 3-chloropropyl itaconate were obtained by esterification of itaconic acid with the corresponding alcohols using *p*-toluensulphonic acid as catalyst. Monomers were characterized by F.T.I.R. and ^{1}H NMR as previously reported [17]. Polymerization is carried out in benzene solutions using AIBN as initiator.

2.2. Dynamic mechanical experiments

Dynamic mechanical measurements were performed by means of a DMTA-MARK II in double cantilever flexural mode. Samples were prepared by moulding the powder of polymers after drying, as probes of $1 \times 10 \times 40$ mm. Samples were dried in oven at least 15 days in order to remove moisture or low molecular weight compounds. Measurements were carried out between 133 and 193 K for PDCEI and 133 to 333 K for PDCPI, at frequencies of 0.3, 1, 3, 10 and 30 Hz.

2.3. Dielectric measurements

Dielectric measurements were carried out on moulded disc-shaped probes with a dielectric analyzer 2970 from TA Instruments. Measurements were carried out at several frequencies between 10^{-1} and 10^5 Hz in the case of PDCEI and from 10^{-2} and 10^5 Hz in the case of PDCPI, in both cases under inert N_2 atmosphere to prevent adsorption of moisture during the experiment.

The experimental uncertainty is better than 5% in all the cases.

2.4. Simulation methodology and computational details

Molecular mechanics studies have been carried out in order to predict the energy associated with a given conformation of a molecule. However, molecular mechanics energies have no meaning as absolute quantities. Only differences in energy between two or more conformations have meaning. Molecular mechanics calculations were performed using the force field method developed by Allinger and co-workers [18,19]. The PC-MODEL software [20] was employed to carry out the calculations. It is based on an empirical force field, called MMX that is derived from MM2(P) [21].

Thus, to adequately express the interaction between atoms inside a polymer, a force field has to possess at least non-bonded, or intermolecular, and intramolecular contributions.

The non-bonded energy function expresses interactions between atoms that are not bonded to each other. It is separated into a van der Waals (a Buckingham potential were employed), the steric component, and a the electrostatic component (interactions between charges, dipoles,…). Parameterization of MMX has been carried out, assuming an artificial dielectric constant of 1.5.

On the other hand, the intramolecular energy function is splitted into a connectivity term, the bond stretching function and flexibility terms, the angle bending and the torsional functions, as well as cross-terms describing the coupling of stretch–bend, bend–bend and torsional–stretch interactions are take into account. The Wilson (E_{OOP}, our umbrella out-of-plane) term has been also included, but their contribution to the global energy was in all cases not extensively studied.

The first step in the calculations is to establish an initial geometry. Exploration of the conformational characteristics of representative skeletal fragments of the polymers is therefore a prerequisite to adequately model larger fragments. The calculations of the theoretical energy requirements for a bond rotation were carried out with two model compounds of one and three-units for each polymer, which simulate part of the polymer chain. Fig. 1 shows the schematic diagram of the two poly(diitaconate)s studied, where the significative angles and distances are indicated.

The conformational energy was calculated as a function of skeletal torsion angles for every 5° in the range from 0 to 360°. The minimization was performed using a combination of Steepest Descent and Newton–Raphson methods [22] till the energy gradient falls below 0.0004 kJ mol^{-1} Å^{-1} for each specific conformer. For each conformational state of the molecular system, the minimization attempts to reach the lowest energy of the system by moving for the atoms all the Cartesian coordinates except those defining the (ϕ_i and ϕ_j) torsion angles. From the conformational energy maps of every backbone torsional pair in the chain, the minima were identified and the relative energies of each minimum were calculated with respect to the global minimum for the particular bond pair. Thus, a set of relative energy values and the corresponding minimum of the torsional energy values for the specific bond pairs in the model compounds were derived.

In spite of the fact that in secondary relaxations in polymers we probably deal with intra- and inter-molecular interactions [23], it should be noted that the present calculations neglect intermolecular interactions. In fact, the calculation of the intermolecular contribution to secondary loss processes in glassy polymers is very difficult. Further, we will see that this assumption is consistent with our results.

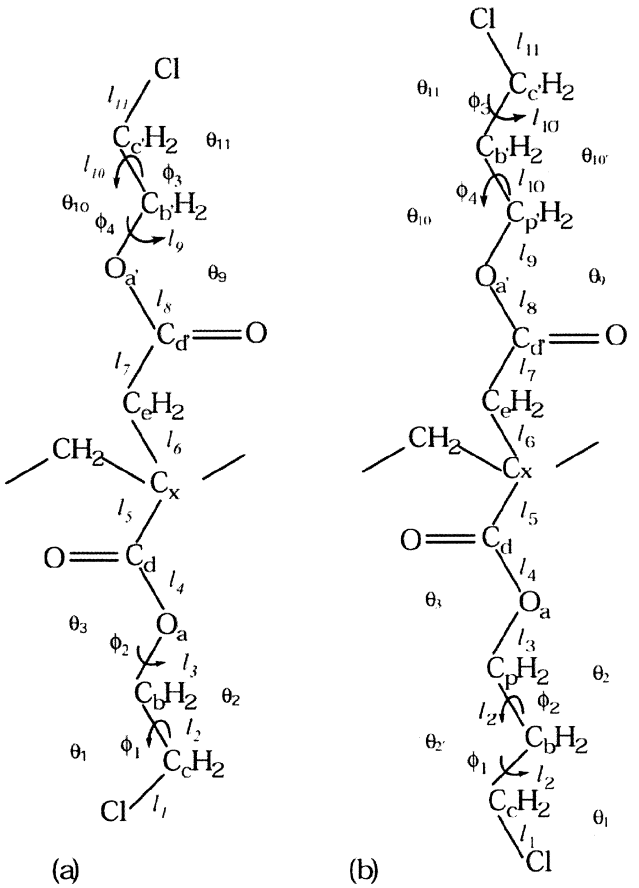

Fig. 1. Schematic diagram of the one-unit model compounds of (a) PDCEI and (b) PDCPI used in the energetic calculations, and definitions of the geometric parameters used in the simulation.

3. Results and discussion

3.1. Dynamic mechanical and dielectric measurements

Fig. 2(a) and (b) shows the storage and loss modulus for both polymers at three frequencies (0.3, 3, and 30 Hz) in the temperature range studied. For sake of clarity, the relaxational data at intermediate frequencies of 1 and 10 Hz are not included. The storage modulus was only represented at 3 Hz. These Figures clearly shows the existence of three main relaxations. About 153 K a first relaxation process can be observed and labeled as γ relaxation. The activation energies, calculated from an Arrhenius plot (Fig. 3) are 37.5.0 ± 0.5 and 36.5 ± 0.5 kJ mol^{-1}, respectively. These values are very similar to that found for other poly(itaconate)s [1–4]. Between 213 and 253 K we observe a broad relaxation labeled as β relaxation. The activation energies according to the Arrhenius equation are 150 ± 5 and 160 ± 5 kJ mol^{-1}, respectively. A third relaxation, probably associated to the glass transition is observed at 316 K for PDCEI and at 295 K for PDCPI at the frequency of 3 Hz. Owing the narrow frequency range of the measurements, the Arrhenius plot gives 284 ± 5 and 192 ± 5 kJ mol^{-1}, respectively for the activation energies. It is well known that the relaxations associated to the glass transition follow a behavior defined by the Williams–Landel–Ferry (WLF) equation. However, in our case, the narrow range of frequencies precludes a WLF analysis and the Arrhenius plot should give a rough indication of the apparent activation energy for these phenomena.

It is interesting to note that, as in other poly(itaconate)s [2,3], the intensity of the α peak expressed in terms of the maxim of the loss modulus appears to be somewhat lower than the intensities of the β or the γ peaks. In general, this behavior is opposite to the usual one; namely, the α relaxation peak is the most prominent of those observed in amorphous polymers [24].

The results corresponding to dielectric relaxations measurements for PDCEI and PDCPI are shown in Fig. 4(a) and (b), respectively. These figures show the dielectric permittivity and loss for the polymers under study at several frequencies (10^x Hz, with $x = 0, 1, 2, 3, 4$). The real part of the complex permittivity is only shown at one frequency for

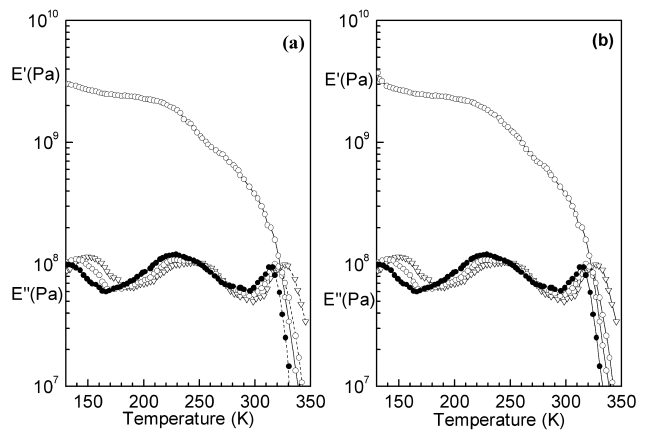

Fig. 2. Storage and loss modulus as a function of the temperature at 0.3 (●), 3 (○) and 30 (▽) Hz for (a) PDCEI and (b) PDCPI.

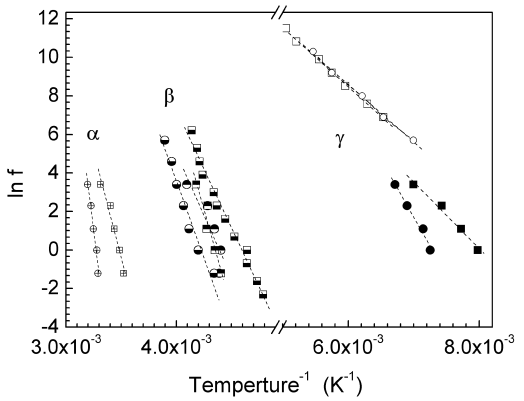

Fig. 3. Arrhenius plot for the γ-relaxation (●, mechanical results of PDCEI, ○ dielectric results of PDCEI, ■ mechanical results of PDCPI, □ dielectric results of PDCPI), β-relaxation (◓ mechanical results of PDCEI, ◒ dielectric results of PDCEI, ⬒ mechanical results of PDCPI, ⬓ dielectric results of PDCPI) and α-relaxation (⊕ mechanical results of PDCEI, ⊞ mechanical results of PDCPI).

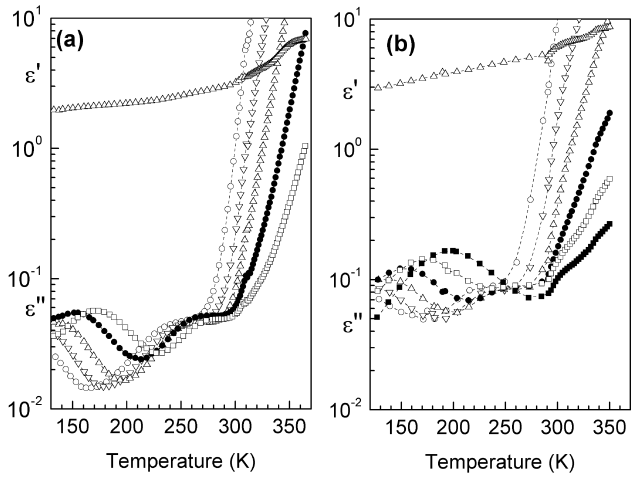

Fig. 4. Experimental permittivity and loss factor at several frequencies (○ 10^0 Hz, ▽ 10^1 Hz, △ 10^2 Hz, ● 10^3 Hz, □ 10^4 Hz) as a function of the temperature for (a) PDCEI, and (b) PDCPI.

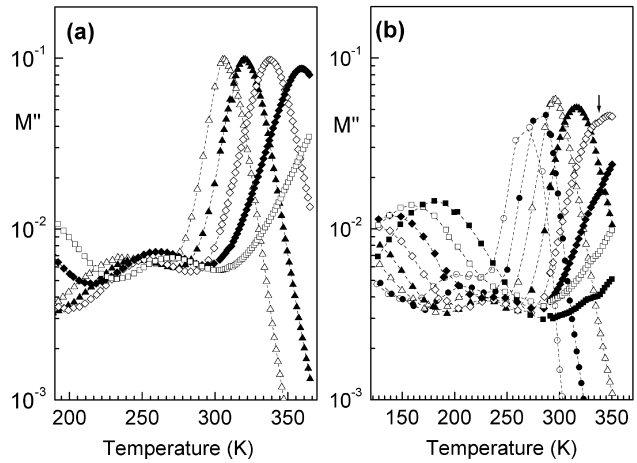

Fig. 5. Electric loss modulus at different frequencies (○ 10^{-2} Hz, ● 10^{-1} Hz, △ 10^0 Hz, ▲ 10^1 Hz, ◇ 10^2 Hz, ◆ 10^3 Hz, □ 10^4 Hz, ■ 10^5 Hz) as a function of temperature for (a) PDCEI, and (b) PDCPI.

sake of clarity. In both spectra we can clearly observe two relaxational zones. When the temperature increases, a peak is observed at 173 K (10^4 Hz), which can be related to the γ mechanical relaxation. Activation energy calculated from an Arrhenius plot (see Fig. 3) is 22 ± 1 kJ mol^{-1} for both polymers. At higher temperatures another relaxation, labeled β relaxation, is also observed. This relaxation overlaps with the high temperature tail of the loss permittivity as observed in many polymers. This fact precludes the appearance of the α relaxations in contrast to that observed in mechanical measurements. On the other hand the overlapping of the conductivity in PDCEI impedes an accurate calculation of the activation energy of the β relaxation in this polymer. For this reason only a roughly estimated value of the activation energy for the β relaxation for PDCEI and PDCPI can be obtained as ~135 kJ mol^{-1}, in both cases. This phenomenon, involving a continuous increase of the loss permittivity when the temperature goes up, suggests the presence of important conductivity contributions (probably a combination of bulk conduction and interfacial polarization effects) that are dominant in the dielectric response. However, some clarification of this fact could be obtained by using the electric modulus formalism ($M^* = (\varepsilon^*)^{-1}$) for the representation of the data. Values of M'' as a function of temperature are shown in Fig. 5(a) and (b). A careful inspection of the curve corresponding at the frequency of 10^2 Hz, represented in Fig. 5(b) shows a shoulder close of the maximum of the peak, at high temperature, presumably associated with the superposition of the dipolar relaxation with the conductive processes. These results, expressed in terms of M'' vs. log ω, give peaks whose halfwidths (at 323, 333 and 343 K) are respectively 1.56, 1.57, 1.63 for PDCEI and 1.68, 1.68, 1.70 for PDCPI. These values are significantly higher than that corresponding to a single Debye peak (1.144). Owing to the fact that pure conductive phenomena are usually well described by a single Debye peak, the values found for the halfwidth, suggest that both interfacial and free charge conductive processes are present, together with dipolar reorientations, in the glass–rubber transitional zone.

It is interesting to note that γ and β dielectric relaxations have lower activation energies than the corresponding mechanical counterparts. This is consistent with the highest temperature at which mechanical relaxation peaks are seen in comparison with the dielectric ones [25]. An interrelationship between dielectric and mechanical spectroscopy was recently discussed in detail by Pakula [26].

In order to characterize and to analyze the mechanical and dielectric spectra in a more detailed way the observed relaxations, it is convenient to choose a model, which appropriately reproduce the experimental data. A reliable model to represent the secondary relaxations in polymers is the Fuoss and Kirkwood equation [27]. This semi-empirical model has been extensively used in the representation of the mechanical and dielectric relaxations and can be written as

$$\Gamma'' = \Gamma''_{\max} \operatorname{sech} mx \tag{1}$$

where Γ'' represents the mechanical/dielectric loss and $\Gamma''_{\max}$ is the value of these quantities at the maximum of the peak, $x = \ln(f_{\max}/f) = (E_a/R)(1/T - 1/T_{\max})$, $T_{\max}$ and $f_{\max}$ are respectively the temperature and frequency. Γ'' has a maximum value given by ($\Gamma''_{\max}$), E_a is the apparent activation energy, R is the gas constant, and m is a parameter ($0 < m < 1$) related to the broadness of the relaxation in the sense that the lower m, the wider the distribution is. The value of $m = 1$ corresponds to a single relaxation time (Debye peak). The strength of the mechanical/dielectric relaxation peak can be calculated from the relationship [28], $\Gamma''_{\max} = m\Delta\Gamma/2$, where $\Delta\Gamma$ represents $E_0 - E_\infty$ and $\varepsilon_0 - \varepsilon_\infty$ for the mechanical and dielectric relaxations, respectively.

In order to calculate the parameters $\Delta\Gamma_\gamma$ and m_γ a variation of the parameters with the frequency from isochrones was performed instead of a variation of these

parameters with temperature from isotherms. The obtained values for dielectric and mechanical γ relaxations summarized in Table 1 are in the same order as those obtained for other poly(itaconate)s [1–4]. The values of m_γ parameter do not show a noticeable dependence on the frequency of the isochrones, and on the temperature of the isotherm. The low values obtained, in both cases, for this parameter seem to be an indication of the distributed character of the process.

In the case of mechanical data, because of the narrow range of frequencies and the flat-shape of the curves for the β relaxation, this procedure is not so accurate. In the dielectric case the problem arises from the overlapping of the conductivity contribution to the β relaxation as was mentioned above. However, a rough estimation of the m parameter and the strength of the relaxation gives $m_\beta = 0.096 \pm 0.014$ and $\Delta E_\beta = 2.28 \times 10^9 \pm 3.44 \times 10^8$ GPa for PDCEI and $m_\beta = 0.091 \pm 0.014$ and $\Delta E_\beta = 3.32 \times 10^9 \pm 5.03 \times 10^8$ GPa for PDCPI at 243 K. These values of m_β are of the same order of magnitude as those obtained for other poly(itaconate)s [1–4]. The low value of the m parameter, in both poly(diitaconate)s, seems to be an indication of the distributed character of this process.

In all cases we have assumed symmetry in the relaxations peaks. However the asymmetric character of the relaxations associated to the glass transition temperature is well known. For this reason another empirical model have been used in order to analyze these relaxations. In this case, the frequency dependences of ε'' can be described by the Havriliak–Negami (HN) empirical expression [29,30]

$$\frac{\varepsilon^*(\omega) - \varepsilon_\infty}{\varepsilon_0 - \varepsilon_\infty} = [1 + (i\omega\tau_0)^{1-\alpha}]^{-\beta} \tag{2}$$

where ε_∞ is the relaxated permittivity, ε_0 is the unrelaxated permittivity, the parameters α and β $[0 < ((-\alpha), ((-\alpha)\beta \leq ()]$ define the symmetrical and asymmetrical broadening of the loss peak, respectively, τ_0 is the relaxation time, and $f_{max} = 1/2\pi\tau_0$ is the characteristic frequency at which ε'' passes through the maximum. The splitting of Eq. (2) in real and imaginary parts gives

$$\varepsilon'(\omega) - \varepsilon_\infty = r^{-\beta/2}(\varepsilon_0 - \varepsilon_\infty)\cos\beta\theta \tag{3a}$$

$$\varepsilon''(\omega) = r^{-\beta/2}(\varepsilon_0 - \varepsilon_\infty)\sin\beta\theta \tag{3b}$$

where

$$r = [1 + (\omega\cdot\tau_0)^{1-\alpha}\cdot\sin(\alpha\cdot\pi/2)]^2[1 + (\omega\cdot\tau_0)^{1-\alpha}\cdot\cos(\alpha\cdot\pi/2)]^2,$$
$$\theta = \operatorname{arctg}\left[\frac{(\omega\cdot\tau_0)^{1-\alpha}\cdot\cos(\alpha\cdot\pi/2)}{1 + (\omega\cdot\tau_0)1 - \cdot\alpha\sin(\alpha\cdot\pi/2)}\right] \tag{4}$$

In order to take into account the conductive contributions to the loss permittivity a hopping model is assumed, and consequently a term $(A/\varepsilon_{vac})\cdot\omega^{-s}$ can be added to Eq. (3b) to

Table 1
Values of m_γ parameter of the Fuoss–Kirwood equation and the strength $\Delta I(\Delta E, \Delta\varepsilon)$ of the γ relaxation process for PDCEI and PDCPI

	PDCEI				PDCPI			
	ΔE (GPa)	m_γ	$\Delta\varepsilon$	m_γ	ΔE (GPa)	m_γ	$\Delta\varepsilon$	m_γ
128 K							1.00	0.214
138 K							1.06	0.207
143 K			0.54	0.254				
148 K			0.53	0.265			1.10	0.216
153 K			0.51	0.279				
158 K			0.51	0.283			1.18	0.214
163 K			0.51	0.283				
170 K							1.21	0.227
173 K			0.48	0.310			1.15	0.258
1×10^5 Hz							1.38	0.224
5×10^4 Hz							1.43	0.213
2×10^4 Hz							1.43	0.199
3×10^4 Hz			0.51	0.295				
1×10^4 Hz			0.51	0.29			1.41	0.188
5×10^3 Hz							1.41	0.181
3×10^3 Hz			0.64	0.26				
2×10^3 Hz							1.40	0.170
1×10^3 Hz			0.52	0.272			1.47	0.152
3×10^1 Hz	1.22×10^9	0.190			1.50×10^9	0.219		
1×10^1 Hz	1.23×10^9	0.180			1.62×10^9	0.200		
3×10^0 Hz	1.26×10^9	0.170			1.58×10^9	0.196		
1×10^0 Hz	1.21×10^9	0.180						

($m_\gamma \pm 0.05$), (ΔE(GPa) $\pm 3.40 \times 10^8$); ($m_\gamma \pm 0.020$), ($\Delta\varepsilon \pm 0.03$).

give

$$\varepsilon''(\omega) = r^{-\beta/2}\cdot(\varepsilon_0 - \varepsilon_\infty)\cdot\sin\beta\theta + \frac{A}{\varepsilon_{vac}}\cdot\omega^{-s} \quad (5)$$

where A is a constant, $s \leq$ and ε_{vac} is the vacuum permittivity [31]. By this way the ε'' frequency dependences were described as a HN process added to a hopping conductivity term. The values of the HN parameters obtained for both polymers, PDCEI and PDCPI, are summarized in Table 2. The quality of the fit is shown in the Fig. 6, where the frequency dependence of ε'' for (a) PDCEI at 333 K and (b) PDCPI at 313 K is illustrated. Lines represent the result of the fit according to the Eq. (5).

The values compiled in Table 2 indicate that the conductivity parameters and HN parameters for both polymers are of the same order of magnitude for both polymers under study.

It is interesting to compare the dynamic mechanical and dielectric data of the polymers under study with those of poly(dipropyl itaconate) (PDPI) and poly(dibutyl itaconate) (PDBI) previously reported [1]. In fact PDCEI and PDCPI results by the insertion of chlorine in the two terminal methylene groups in the lateral chains. In Fig. 7(a) the mechanical loss tangent of PDPI and PDCEI at 1 Hz are compared. In the same way in Fig. 7(b) the loss tangent of PDBI and PDCPI at 1 Hz are also compared. The most important differences between these two sets of data appear in the low temperature side of the curves. Two subglass γ and β relaxations are shown in the chlorine containing polymers in contrast with the mostly flat curves in the case of the PDPI and PDBI. Dielectric loss tangent at 1 Hz. (Fig. 7(c) and (d)), also show important differences between chlorine and chlorine-free polymers. Firstly, in the case of PDCEI and PDCPI the α relaxations are contaminated by conductive effects, and for this reason at this frequency only appears as a shoulder in the experimental curves. In contrast, the data of PDPI and PDBI show clearly the α relaxation. With respect to the low temperature relaxations, it is also evident that the loss tangent is more clearly defined and higher in the case of chlorine containing polymers. The only exception seems to be the β relaxation of PDBI and PDCPI that shows similar intensities. According to these features, it seems to be clear that the chlorine atoms are the responsible for the appearance of the γ relaxations in

Table 2
Havriliak–Negami fit parameters for PDCEI and PDCPI at 333 and 313 K, respectively, from the $\varepsilon''(\omega)$

	PDCEI	PDCPI
$\Delta\varepsilon$	2.151	2.540
α	1	1
β	0.288	0.1431
τ_{HN}	2.19×10^{-2}	4.26×10^{-2}
A	7.51×10^{-9}	1.94×10^{-9}
s	0.9533	0.904

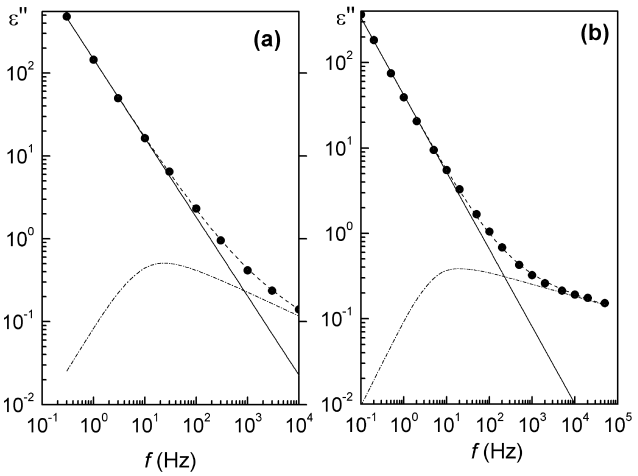

Fig. 6. Frequency dependence of ε'' for (a) PDCEI at 333 K and (b) PDCPI at 313 K. Experimental data (•); lines represent the result of the fit, according with the Eq. (5). Calculated curve (- -), calculated contribution of the conductive (—) and dipolar relaxation (- • -).

PDCEI and PDCPI. Moreover, these chlorine atoms appear to be also active in the more complex motions causing the β relaxations. It seems reasonable to assign the β relaxations to motions of the lateral chains of the polymers as a whole involving librations of the dipolar groups existing in these chains.

3.2. Molecular mechanics study of γ-relaxation

We will now make a tentative interpretation of the molecular origin of the observed secondary γ relaxations. In order to relate the experimental relaxational processes with motions of the parts of the polymers, we will now compare the calculated conformational energy barriers with the activation energies, E_a, obtained from dielectric and mechanical relaxations measurements. The optimized geometry of the one-unit model (monomer) compound of PDCEI and PDCPI, calculated by force field MMX is plotted in Fig. 8. The size of the total energy requirements for overall rotations about the bonds C_b–C_c, $C_{b'}$–$C_{c'}$, C_d–O_a, $C_{d'}$–$O_{a'}$ and $C_{p'}$–$O_{a'}$, of the molecules shown in Fig. 1

Table 3
Energy requirements (in kJ mol^{-1}) for one-unit models of the PDCEI and PDCPI for complete rotation about the given bond

PDCEI		PDCPI	
C_b–C_c	25.21	C_b–C_c	35.74
C_b–O_a	119.34	C_b–C_p	15.80
O_a–C_d	1036.6	C_p–O_a	138.82
C_d–C_x	5.48	O_a–C_d	1437
C_e–$C_{d'}$	35.82	C_d–C_x	12.52
$C_{d'}$–$O_{a'}$	67.38	C_e–$C_{d'}$	91.87
$O_{a'}$–$C_{c'}$	118.13	$C_{d'}$–$O_{a'}$	325.45
$C_{b'}$–$C_{c'}$	26.33	$O_{a'}$–$C_{p'}$	137.10
		$C_{p'}$–$C_{b'}$	16.39
		$C_{b'}$–$C_{c'}$	35.78

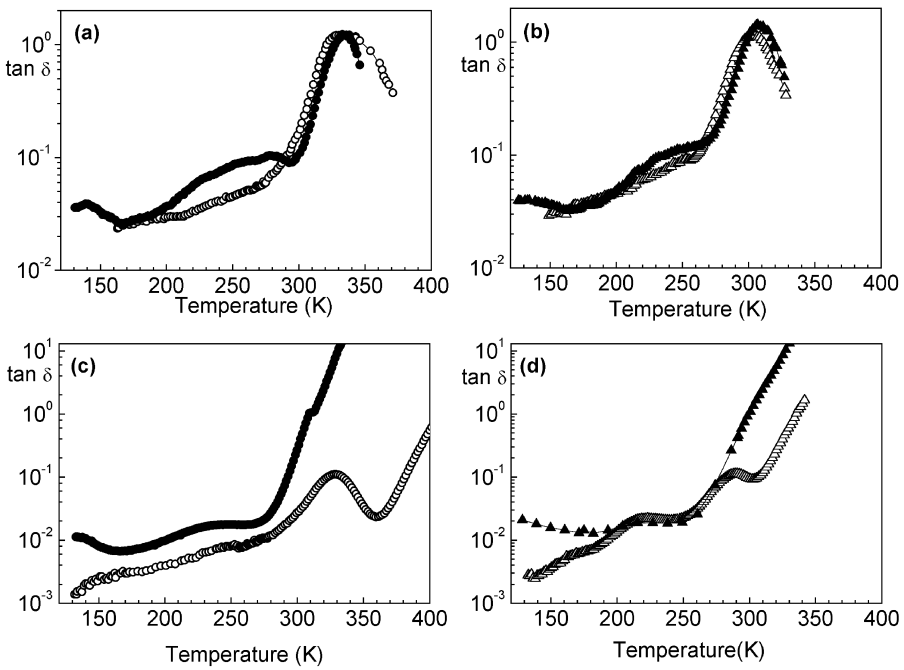

Fig. 7. Mechanical loss tangent at 1 Hz of (a) PDPI (○) and PDCEI (●) and (b) PDBI (△) and PDCPI (▲); loss tangent of (c) PDPI (○) and PDCEI (●) and (d) PDBI (△) and PDCPI (▲).

are shown in Table 3. The geometrical parameters including the bond lengths and bond angles (described in Fig. 1) were derived from the force field optimized geometries of the corresponding repeat units and these are listed in Table 4.

According to the previous results, in order to interpret the molecular motions responsible for the γ transition, the molecular mechanics calculations were carried out on two model compounds of one and three units. A diagram of the one-unit model compounds used is shown in Fig. 1, with the two relevant pair of the torsion angles (ϕ_1, ϕ_2) and (ϕ_3, ϕ_4). The one-unit model (monomer) compounds were used to study the behavior of the side groups without interference from other side groups. In order to take into account the interactions between different side groups and to obtain more realistic results, also the three-unit model were analyzed. The calculations were confined to the rotation around the C_b-C_c ($C_{b'}-C_{c'}$) bond, because previous calculations showed that the barriers of the other bonds are too high to be related to the γ relaxation, which at present is the subject of our study.

Fig. 9 shows the iso-energy contour maps for the monomer model compound of PDCEI and PDCPI as a function of (ϕ_1, ϕ_2) and (ϕ_3, ϕ_4) bond pairs, for the one-unit models. The iso-energy contours are at interval of 2 kJ mol^{-1}. In each calculation the specified pair of dihedrals is constrained at certain desired values and the rest of the structure is allowed to move freely to minimize energy. From the conformational energy maps obtained for every distinct backbone torsional pair in these polymers, the minima of energy were identified and the relative energies of each minimum were calculated with respect to the global minimum for the particular bond pair. Relative energy values and the corresponding minimum energy torsional

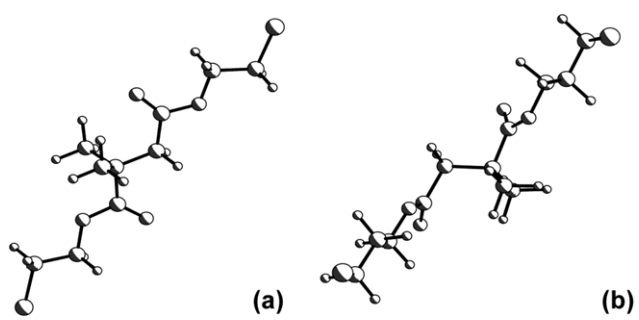

Fig. 8. Geometry optimized conformations of the repeat unit of the poly(diitaconates) studied (a) PDCEI and (b) PDCPI.

Table 4
Geometrical parameters (l_i; (Å) and θ_i, ϕ_i; (°)) derived from the FF-optimized geometries of PDCEI and PDCPI one-unit model compounds

	PDCEI	PDCPI		PDCEI (°)	PDCPI (°)
l_1	1.787	1.787	θ_1	111.102	111.202
l_2	1.530	1.533	θ_2	107.886	110.946
$l_{2'}$		1.534	$\theta_{2'}$		108.369
l_3	1.409	1.409	θ_3	121.773	121.762
l_4	1.343	1.341	θ_9	121.955	121.581
l_8	1.344	1.342	θ_{10}	107.734	108.416
l_9	1.409	1.409	$\theta_{10'}$		110.941
$l_{10'}$		1.534	θ_{11}	111.098	111.92
l_{10}	1.531	1.533	ϕ_1	180	179.974
l_{11}	1.787	1.787	ϕ_2	180	179.957
			ϕ_3	180	179.933
			ϕ_4	180	179.859

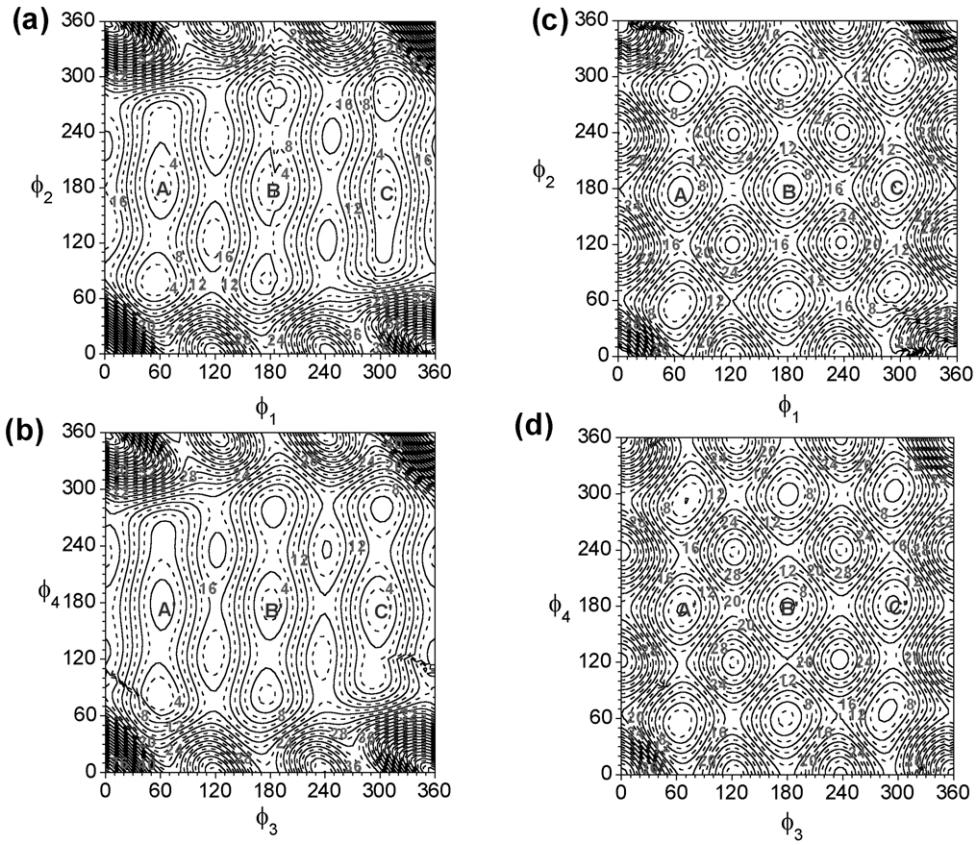

Fig. 9. Contour maps of the conformational energy for (a,b) PDCEI and (c,d) PDCPI at 300 K as a function of the rotation angles (ϕ_1, ϕ_2) and (ϕ_3, ϕ_4). Local minima are shown at B, (B′) and the iso-energetic curves reported as kJ mol^{-1} are spaced 2 kJ mol^{-1}.

values for the specific bond pairs in these poly(diitaconate)s were then estimated from the corresponding iso-energy contours.

As shown in Fig. 9(a) and (b), the rotations about the (ϕ_1, ϕ_2) and (ϕ_3, ϕ_4) bond pairs in PDCEI lead to various minimum energy torsional states corresponding to (~60°, 180°), (180°, 180°), (~300°, 180°), (180°, ~90°) and (180°, ~270°). The region around $\phi_2 = 0$ to 60° ($\phi_1 = 0$ to 360°) and $\phi_2 = 300$ to 360° ($\phi_1 = 0$ to 360°) is probably inaccessible because of severe steric hindrance between the carbonyl oxygen and the terminal chloride of the ethyl group. The minimum energy of torsional states for bonds ϕ_1 and ϕ_3 correspond to 60, 180 and 300°.

Moreover, as shown in Fig. 9(c) and (d), the rotations about the ($\phi_($, ϕ_2) and (ϕ_3, ϕ_4) bond pairs in PDCPI lead to various minimum energy of torsional states corresponding to (~60°, 60°), (60°, 180°), (60°, ~280°), (180°, 60°), (180°, 180°), (180°, 300°) (300°, ~70°) and (300°, ~300°). In this case, also we can observe that the regions around (0°, 0°), (0, 360°), (360°, 0°) and (360°, 360°) are inaccessible on this occasion because of steric hindrance between the carbonyl oxygen and the terminal chlorine of the propyl group.

These plots are useful in analyzing the conformations, and transitions paths of different moieties of the polymer. So, the most probable path of rotation responsible of the γ relaxation is A ↔ B ↔ C ↔ A and A′ ↔ B′ ↔ C′ ↔ A′, in which ϕ_2 and ϕ_4 is kept almost constant (~180°).

The energy barrier for ϕ_1 and ϕ_3 bond of the PDCEI, as derived using Force Field MMX in our present study, is ~26.3 kJ mol^{-1}, which is close to that derived from dielectric and mechanical relaxations measurements (22.2 and 37.6 kJ mol^{-1}, respectively). In the case of PDCPI, the energy barrier for ϕ_1 and ϕ_3 bonds derived from the MMX program is ~35.7 kJ mol^{-1}, which is also close to that derived from dielectric (22.2 kJ mol^{-1}) and mechanical (36.8 kJ mol^{-1}) relaxations measurements. It is possible that the broadening of the γ peak (low value for the m_γ parameter) could be due to an overlapping of two independent rotations of each terminal $\cdots CH_2-CH_2Cl$ group.

Typical energy profiles for the conformational transitions of selected side groups are shown in Figs. 10. This Figure shows the minimum static conformational energy (in kJ mol^{-1}) as a function of the torsion angle of the lateral units. Each group rotation shows a specific energy profile, which depends on the local environment of the group. In our case, in all cases the shape of the energy profiles obtained are very similar. Three energy minima, very similar in energy, can be seen on the plots. Moreover, two successive conformational path performed of the same side group have

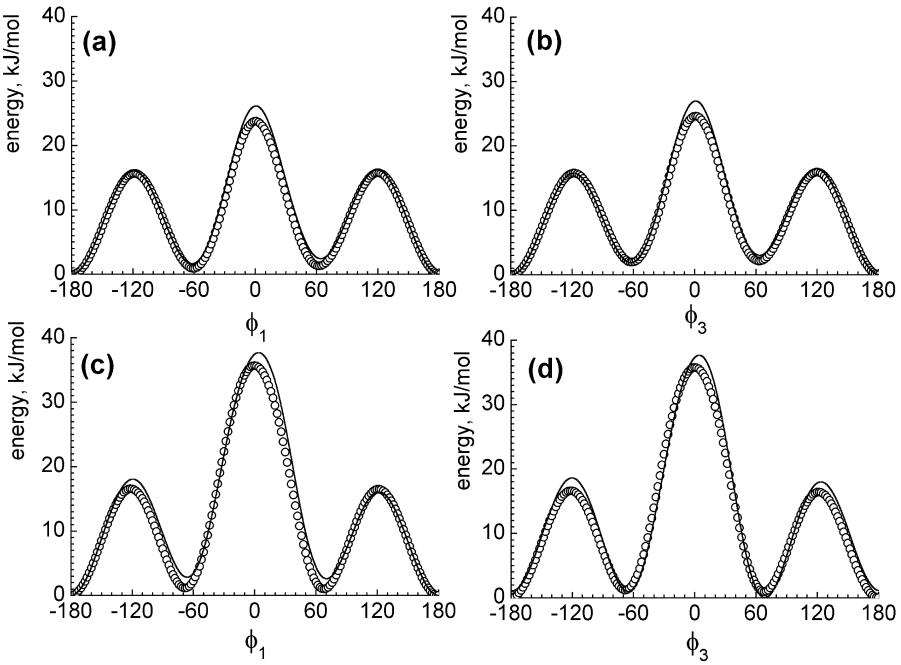

Fig. 10. Potential energy (kJ mol^{-1}) profile for rotation of C_b-C_c bond (ϕ_2, $\phi_4 = 180°$) for (a), (b) PDCEI and (c), (d) PDCPI model compounds. [(○) one- unit model and (—) three-unit model].

the same trace after two or three successive rotations of 360°. Finally, the shape of the energy profiles obtained by positive increments is the same as those obtained with negative increments. This should ensure the reversibility of the quasi-static process. Independent of the polymers, the variations of the torsion angle studied have little consequences on the remaining part of the chain. The side group motions can occur without simultaneous conformational variations of the polymer. The motions of both side groups remain localized, and this suggests an absence of cooperativity. Indeed, the reversibility of the quasi-static process can be related to the non-cooperative character of the relaxation.

Overall, the activation energies calculated from the structures from molecular dynamic are not exactly equal than those measured by dielectric and mechanical measurements. Part of this difference might still be due to inadequate chain conformation in the generated structures, this difference may also be partially attributed to the static nature of the simulation in which the effect of the bonds non directly connected not it is taken into account.

The next relaxation, which has been observed when moving to higher temperatures in both poly(diitaconate)s, is here designated the β process. The very low value of the m_β parameter obtained by fitting the dielectric measurements at the Fuoss and Kirkwood empirical model indicated that this relaxation is cooperative and for this reason it is difficult to assign the energy activation energy to a single energy barrier, this activation energy is the result of the contributions of different motions. According with the results summarized in Table 3 it is possible to attribute the molecular origin of this relaxation at the rotation of the OCO—alkyl group. However, the participation of the main-chain cannot be disregarded as in poly (itaconate)s and closely related poly (methacrylate)s [3,8–12,32,33].

4. Conclusions

The relaxational behavior of the two poly(di-*n*-chloroalkylitaconate)s studied, indicates that at least three relaxations are observed in the range of frequencies and temperatures studied.

The molecular mechanics calculations strongly support the idea that the molecular mechanism of the γ relaxation is a limited rotation around the C_b-C_c ($C_{b'}-C_{c'}$) bond. The energy map for the (ϕ_1, ϕ_2) and (ϕ_3, ϕ_4) bond pair shows that the C_b-C_c ($C_{b'}-C_{c'}$) could rotate from −180 to 180° with an energy barriers of ~25.20 kJ mol^{-1} (PDCEI) and ~35.78 kJ mol^{-1} (PDCPI), when the ϕ_2 and ϕ_4 groups are restricted to 180°. This implies a higher intramolecular flexibility for the terminal chloroalkyl group.

We have shown that the results obtained are in good qualitative agreement with other calculations, and experimental results available in the literature. This indicates that the intermolecular interactions are negligible. Moreover, the values obtained employing one-unit and three-unit model compounds are very similar, indicating that the length of the chain is not a determining factor in the activation energy associated with the relaxation under study. The motion can occur without rearrangement of the backbone. This is in agreement with the hypothesis of a localized and

non-cooperative relaxation. Motions of the type studied are supposed to be the easiest in terms of energy cost.

In the PDCEI the conformations (0°, 0°), (0°, 360°), (360°, 0°) and (360°, 360°) were found to be a higher energy of $\sim 98\ \mathrm{kJ\ mol^{-1}}$ due to the interactions between the carbonyl oxygen and the chloroethyl group. In the case of the PDCPI the same conformations were found to be energy of $\sim 58.5\ \mathrm{kJ\ mol^{-1}}$ (PDCPI). The lower values obtained in the case of PDCPI could be associated at the higher distance between the carbonyl oxygen and the chlorine group. So, the long sequences of $-CH_2-$ of the *n*-alkyl side group give rise to a variety of degrees of freedom that can be responsible of the values of the m_γ parameter summarized in Table 1 for the two poly(diitaconate)s shows that $m_\gamma(\mathrm{PDCEI}) > m_\gamma(\mathrm{PDCPI})$. The lower value of m_γ for the PDCPI could be associated to the contribution of the rotation of the C_b-C_p absent in PDCEI. In this sense, Shimizu et al. [13] suggest that in the case of PnBMA there are two coupled peaks assigned to the rotation of the *n*-propyl group and the terminal ethyl group.

The barriers calculated by molecular mechanics calculations in these poly(diitaconate)s are somewhat higher than those corresponding to poly(chloroethyl methacrylate) (PCEMA) and poly(chloropropyl methacrylate) (PCPMA) reported previously [14]. Probably, this is originated from the fact that, in the poly(diitaconate)s, there are, instead of CH_3- and $-CO_2R$ groups at both side of main-chain, two bulkier $-CO_2R$ groups. For this reason, we can expect that, in our case, the steric hindrance to the motions should be larger.

Moreover, dynamic mechanical experiments of PDCEI and PDCPI show a very broad peak corresponding to the secondary β-relaxation with apparent activation energy of $\sim 135\ \mathrm{kJ\ mol^{-1}}$ and a short pre-exponential time ($\sim 10^{-40}$ s), which indicates a certain motional cooperativity [34]. When a relaxation is cooperative, and this is the case for the β-relaxation, it is difficult to assign the apparent activation energy to a single energy barrier. The averaging of the activation energies is the result of the contributions of different motions. For those reasons, a direct comparison between calculated and experimental results remains qualitative. It supports the idea of the precursor character of the β-relaxation with respect to the glass transition. By this way, Cowie and Ferguson [10] have reported a study on molecular dynamics in poly(methacrylate)s and poly(di-*n*-alkyl itaconate)s. These authors have indicated that the β relaxation could be due to the oxycarbonyl group, but only some cooperation from the main-chain could not be disregarded. These conclusions are in agreement with the Heijboer's [8] work for PMMA.

Although α relaxation is clearly apparent in mechanical data, the intensity of these peaks appears to be lower in terms of the loss module than those of β relaxation. This can be due to the versatility of the chains of these polymers whose molecular motions are mainly activated in γ and β relaxations. Moreover, dielectric α relaxational zone is highly contaminated by conductive phenomena and for this reason convenient strategies, in terms of the electric modulus and hopping conductivity terms, have been developed to analyze this zone.

Acknowledgements

MJSS and RDC gratefully acknowledge to CICYT for grant MAT2002-04042-C02-01. L.G. and D.R. acknowledge to FONDECYT Grants 1010478 and 1010726 for financial help.

References

[1] Díaz Calleja R, Gargallo L, Radic' D. Macromolecules 1995;28(20):6963–9.
[2] Díaz Calleja R, Sanchis MJ, Gargallo L, Radic' D. J Polym Sci Polym Phys 1996;34(2):261–6. Díaz Calleja R, Sanchis MJ, Gargallo L, Radic' D. J Polym Sci Polym Phys 1997;35(16):2749–56.
[3] Díaz Calleja R, Saíz E, Riande E, Gargallo L, Radic' D. J Polym Sci Polym Phys 1994;32(6):1069–77. Díaz Calleja R, Saíz E, Riande E, Gargallo L, Radic' D. Macromolecules 1993;26(15):3795–802. Díaz Calleja R, Saíz E, Riande E, Gargallo L, Radic' D. J Non-Cryst Solids 1994;172:985–9.
[4] Ribes-Creus A, Díaz Calleja R, Gargallo L, Radic' D. Polymer 1991;32(15):2755–9. Ribes-Creus A, Díaz Calleja R, Gargallo L, Radic' D. Polymer 1991;32(13):2331–4.
[5] Díaz Calleja R, Pelissou O, Gargallo L, Radic' D. Polymer 1994;35(13):3449–55.
[6] Flory PJ. Statistical mechanics of chain molecules. New York: Interscience; 1969.
[7] Mattice WL, Suter UW. Conformational theory of large molecules. New York: Wiley; 1994.
[8] Heijboer J, Baas JMA, van de Graaf B, Hoefnagel MA. Polymer 1987;28(3):509–13. Heijboer J, Baas JMA, van de Graaf B, Hoefnagel MA. Polymer 1992;33(7):1359–62.
[9] Heijboer J. Makromol Chem A 1960;35:86.
[10] Cowie JM, Ferguson R. Polym Commun 1984;25(3):66–8. Cowie JM, Ferguson R. Polymer 1987;28(3):503–8.
[11] Cowie JM, Mc Ewen IJ. Macromolecules 1981;14(5):1374–7. see also 1378–1381.
[12] Baas JMA, van de Graaf B, Heijboer J. Polymer 1991;32(12):2141–5.
[13] Shimizu K, Yano O, Wada Y. J Polym Sci 1975;13(10):1959–74.
[14] Esteve-Marcos C, Sanchis MJ, Díaz-Calleja R. Polymer 1997;38(15):3805–10.
[15] De la Rosa A, Heux L, Cavaillé JY, Mazeau K. Polymer 2002;43(21):5665–77.
[16] Sulhata MS, Natajaran U. Macromol Theory Simul 2003;12(1):61–71.
[17] Radic' D, Dañin C, Opazo O, Gargallo L. Makromol Chem Macromol Symp 1992;58:209–13.
[18] Phillip T, Cook RL, Malloy TB, Allinger NL, Chang S, Yuh Y. J Am Chem Soc 1981;103(9):2151–6. Allinger NL, Yuh H. Quantum Chem Prog Exch QCPE 1981;13:395.
[19] Allinger NL, Zhou X, Bergsma J. J Mol Struct (Theochem) 1994;118(1):69–83.
[20] Available from Serena Software, PO Box 3076, Bloomington IN 47402-3076.
[21] Allinger NL, Sprague JT. J Am Chem Soc 1973;95(12):3893–907.
[22] Press WH, Teukolsy SA, Vetterling WT, Flannery BP. Numerical recipes in C, 2nd ed. New York: Cambridge University Press; 1992.

[23] Struik LCE. Molecular dynamics and relaxation phenomena in glasses. In: Dorfmüller T, Williams G, editors. Lectures notes in physics, vol. 277. Berlin: Springer; 1987. p. 27.
[24] McCrum NG, Read BE, Williams W. Anelastic and dielectric effects in polimeric solids. New York: Dover; 1991.
[25] Díaz Calleja R, Sanchis MJ, Gargallo L, Radic' D. Macromol Chem Phys 1995;196(11):3789–96.
[26] Pakula T. In: Kremer F, Schönhals A, editors. Broadband dielectric spectroscopy. Berlin: Springer; 2003. p. 597.
[27] Fuoss R, Kirkwood JG. J Am Chem Soc 1941;63:385–94.
[28] McCrum NG, Read BE, Williams W. Anelastic and dielectric effects in polymeric solids. New York: Dover; 1991. p. 118.
[29] Havriliak S, Negami S. J Polym Sci Part C Polym Symp 1966;14PC: 99.
[30] Havriliak S, Negami S. Polymer 1967;8(1):161–210.
[31] Bottcher CJF, Bordewijk P. Theory of electric polarization, 2nd ed. Amsterdam: Elsevier; 1978. p. 72.
[32] Gómez-Ribelles JL, Díaz-Calleja R. J Polym Sci Polym Phys 1985; 23(7):1297–307.
[33] Díaz Calleja R, Saíz E, Riande E, Gargallo L, Radic' D. Macromolecules 1993;26(15):3795–802.
[34] De la Rosa A, Heux L, Cavaille JY. Polymer 2000;41(20):7547–57.